TU Delft

Delft University of Technology

PMU-Based Backup Protection in the Presence of Inverter-Based Resources

Jegarluei, Mohammad Rezaei; Dobakhshari, Ahmad Salehi ; Popov, Marjan; Terzija, Vladimir; Azizi, Sadegh

DOI
10.1109/ETFG55873.2023.10408512

Publication date
2023

Document Version
Final published version

Published in
Proceedings of the 2023 IEEE International Conference on Energy Technologies for Future Grids (ETFG)

Citation (APA)
Jegarluei, M. R., Dobakhshari, A. S., Popov, M., Terzija, V., & Azizi, S. (2023). PMU-Based Backup Protection in the Presence of Inverter-Based Resources. In *Proceedings of the 2023 IEEE International Conference on Energy Technologies for Future Grids (ETFG)* IEEE. https://doi.org/10.1109/ETFG55873.2023.10408512

Important note
To cite this publication, please use the final published version (if applicable).
Please check the document version above.

Copyright
Other than for strictly personal use, it is not permitted to download, forward or distribute the text or part of it, without the consent of the author(s) and/or copyright holder(s), unless the work is under an open content license such as Creative Commons.

Takedown policy
Please contact us and provide details if you believe this document breaches copyrights.
We will remove access to the work immediately and investigate your claim.

This work is downloaded from Delft University of Technology.
For technical reasons the number of authors shown on this cover page is limited to a maximum of 10.

Green Open Access added to TU Delft Institutional Repository

'You share, we take care!' - Taverne project

https://www.openaccess.nl/en/you-share-we-take-care

Otherwise as indicated in the copyright section: the publisher is the copyright holder of this work and the author uses the Dutch legislation to make this work public.

2023 IEEE International Conference on Energy Technologies for Future Grids
Wollongong, Australia, December 3-6, 2023

2023 IEEE International Conference on Energy Technologies for Future Grids (ETFG) | 978-1-6654-7164-0/23/$31.00 ©2023 IEEE | DOI: 10.1109/ETFG55873.2023.10408512

PMU-Based Backup Protection in the Presence of Inverter-Based Resources

Mohammad Rezaei Jegarluei[a], Ahmad Salehi Dobakhshari[b], Marjan Popov[c], *Fellow*, *IEEE,*
Vladimir Terzija[d], *Fellow*, *IEEE,* and Sadegh Azizi[a], *Senior Member, IEEE*
[a] School of Electronic and Electrical Engineering, University of Leeds, UK
[b] Faculty of Engineering, University of Guilan, Iran
[c] Faculty of Electrical Engineering, Mathematics and Computer Science, Delft University of Technology, Netherlands
[d] School of Electrical Engineering, Shandong University, China
elmrj@leeds.ac.uk; salehi_ahmad@guilan.ac.ir; m.popov@tudelft.nl; vladimir.terzija@yahoo.com; s.azizi@leeds.ac.uk

***Abstract*—Increasing penetration of inverter-based resources (IBRs) undermines the performance of conventional protection systems since IBRs' fault characteristics are fundamentally different from those of synchronous generators. In this paper, a PMU-based backup protection method is proposed for power transmission systems with high penetrations of IBRs. The method involves replacing all IBRs and the line suspected to be faulty by proper nodal current sources. For accurately detecting the faulted line from the set of candidates, a residual-based index is proposed, utilizing the concept of superimposed circuits and the weighted least-squares method. The method's robustness in the face of influential factors, including input errors, settings, numbers, and locations of IBRs is investigated through extensive simulations on the IEEE 39-bus test system.**

***Index Terms*— Inverter-based resource (IBR), synchrophasor, superimposed circuits, wide-area backup protection.**

I. Introduction

RENEWABLES are usually connected to the rest of the electricity grid through power-electronic inverters as interface. This enables inverter-based resources (IBRs) to offer distinguished controllability characteristics and fulfill their control targets within a few milliseconds [1]. IBRs exhibit fundamentally different fault behaviors compared to synchronous generators, making the design philosophies of conventional protections less reliable or even invalid. In addition to the inherent deficiencies of local protection systems, protection problems caused by high penetration of IBRs are evidenced by increasing misoperation/malfunction cases of protection functions [2]-[6].

There has been significant academic interest in the improvement of protection methods, specifically within power systems that integrate a large amount of renewable energy sources [7]-[9]. Wide-area backup protection (WABP) is notably advantageous due to its ability to access a greater number of more accurate measurements compared to conventional local protection methods [10]. The majority of WABP methods proposed thus far have been designed for conventional power systems. Most of these methods suffer from the nonlinearity of formulations and normally rely on a specific set of input phasors and cannot tolerate PMU losses or long communication latencies [11]-[13].

Synchronous generators are modeled as an impedance in series with a voltage source in many WABP methods [14]-[18]. This modeling technique, however, cannot be employed for IBRs because of their distinctive fault behaviors, which calls for innovative solutions. In recent years, some WABP methods have included IBRs. The authors in [19] present a method that complements distance protection by WABP. One major shortcoming of this method is its reliance on specific PMU placements. The method of [20], focuses on transmission systems with a significant presence of IBRs by utilizing negative-sequence components. However, a limitation of this method is that it only accounts for asymmetrical faults.

This paper presents a novel WABP method designed for the protection of power systems in the presence of high-level penetration of IBRs. The method takes into consideration the non-linear behavior and low-voltage ride-through (LVRT) characteristics of IBRs, regardless of their number and placement. In this paper, IBRs are substituted by current sources based on the Substitution Theorem [15], whose values will be either measured by PMUs or obtained based on IBR's Grid Code requirements [21]-[22]. The faulted line is substituted by two unknown nodal current sources, facilitating the estimation of unknown currents through the utilization of the weighted least-squares (WLS) method. A closed-form residual-based index is put forward to determine the validity of estimation, which makes it possible to identify the faulted line amongst candidate ones.

The rest of this paper is structured as follows. Section II describes the common configuration and control strategies of IBRs. The formulation used for faulted line identification is detailed in Section III. Section IV explains the modifications applied to account for the high penetration of IBRs. Simulation results and comparison studies are discussed in Section V. Finally, Section VI puts forward the concluding remarks.

II. Arrangement and Control System of IBRs

This section addresses the configuration and power control strategy applied to IBRs with regard to compliance with Grid Code requirements. Fig. 1 shows the typical arrangement and control system for a voltage source converter as an IBRs. As shown, the inner controller's current references are determined by the outer controller. Then, these are converted to control references used for the PWM controller [1].

The currents and terminal voltages of IBRs are initially expressed in the stationary $\alpha\beta$ frame, from which the positive-

978-1-6654-7164-0/23/$31.00 ©2023 IEEE

Authorized licensed use limited to: TU Delft Library. Downloaded on February 05,2024 at 10:49:11 UTC from IEEE Xplore. Restrictions apply.

sequence quantities are extracted [1]. For example, positive-sequence current quantities in $\alpha\beta$ frame can be calculated as follows:

$$\begin{bmatrix} i_\alpha^+ \\ i_\beta^+ \end{bmatrix} = \frac{1}{2}\begin{bmatrix} 1 & -j \\ j & 1 \end{bmatrix}\begin{bmatrix} i_\alpha \\ i_\beta \end{bmatrix} \quad (1)$$

in which "j" refers to a 90° anticlockwise shift in the phase angle, and the superscript "+" refers to positive-sequence components. Finally, these quantities are converted into the rotating dq frame, i.e. i_d^+ and i_q^+ [1].

As can be seen in Fig.1, in both normal operating conditions and during faults, the primary function of the outer controller entails the regulation of the active and reactive power references. [1]. Grid Codes usually standardize the operation of IBRs during fault conditions, known as LVRT requirements [21]-[22]. To this end, they inject additional positive-sequence reactive current to provide voltage support. Various LVRT requirements are defined in Grid Codes for different IBRs. For instance, Fig. 2 illustrates the reactive current injection of a wind turbine as mandated by reference [21]. It is observed that wind turbines are obligated to inject positive-sequence reactive current that is proportionate to the voltage drop experienced during fault.

III. Identification of the Faulted Line

Using the superimposed circuit methodology presented in [15], a set of linear equations is formulated for each candidate faulted line. This methodology involves substituting the candidate line with two appropriate nodal current sources. Within WABP's time frame of interest, the sub-transient impedance of synchronous generators can serve as a substitute for synchronous generators in the superimposed circuit [12], [15]-[16]. This research paper replaces IBRs by unknown nodal current sources. The weighted sum of squared residuals (*WSSR*s) is utilized for identifying the faulted line, as explained in subsection III-B. It is shown that replacing all IBRs by unknown current sources might excessively increase the quantity of unknowns in the set of equations and raise unsolvability concerns [23]. Then, a method is proposed in Section IV for reducing the number of unknowns.

A. Systems of Equations for Each Candidate Line

Let us assume that a line *i-j* is the faulted line. As can be seen in Fig. 3, $\Delta J_{j,i}^+$, $\Delta J_{i,j}^+$, and ΔI_r^+ are used to denote the superimposed currents of the receiving- and sending-ends of this line, and the IBR at bus *r*, respectively. The superimposed voltage at an arbitrary bus, e.g., bus *q*, in the positive-sequence circuit, can be calculated as below:

$$\Delta V_q^+ = \sum_{r=1}^{Nr} Z_{q,r}^+ \Delta I_r^+ + Z_{q,j}^+ \Delta J_{j,i}^+ + Z_{q,i}^+ \Delta J_{i,j}^+ \quad (2)$$

Where the indices of buses with IBRs are denoted by 1 to *Nr*, and $\boldsymbol{Z}^+$ denotes the bus impedance matrix of the system in the positive-sequence circuit excluding IBRs and line *i-j*.

Let $\Delta J_{u,w}^+$ denote the positive-sequence superimposed current of a healthy line *u-w* at its sending end. This current can be calculated with respect to the nodal current sources as follows:

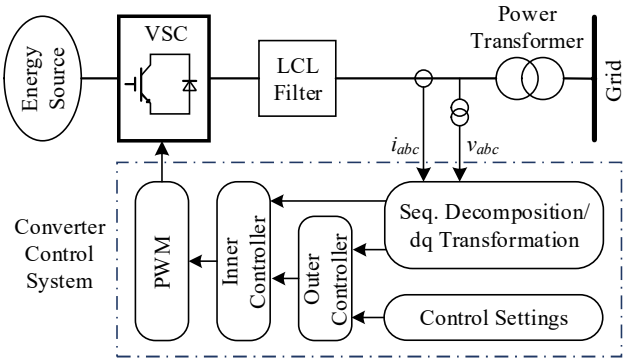

Fig. 1. Common arrangement and control system of IBRs.

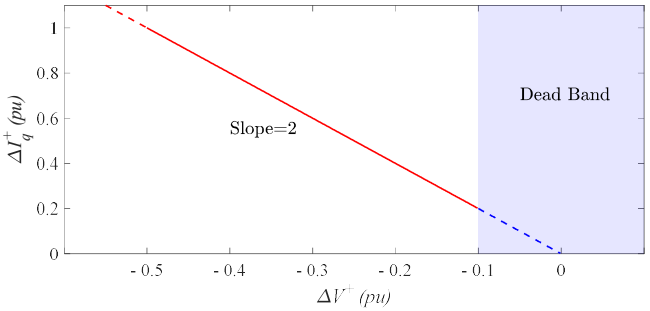

Fig. 2. Reactive current injection requirements for wind turbine in [21].

$$\Delta J_{uw}^+ = \sum_{r=1}^{Nr} C_{uw,r}\, \Delta I_r^+ + C_{uw,i} \Delta J_{i,j}^+ + C_{uw,j} \Delta J_{j,i}^+ \quad (3)$$

The derivation of C_{uw} is presented in [15]. If any superimposed phasors, i.e., ΔV_k^+, ΔJ_{uw}^+, ΔI_r^+, $\Delta J_{i,j}^+$, and $\Delta J_{j,i}^+$ are directly measured by PMUs, the set of equations (4) can be developed for the superimposed synchrophasor measurements acquired:

$$\begin{cases} \Delta V_q^{meas,+} = \Delta V_q^+ + e_{V(k)} \\ \Delta J_{uw}^{meas,+} = \Delta J_{uw}^+ + e_{J(uw)} \\ \Delta I_r^{meas,+} = \Delta I_r^+ + e_{I(r)} \\ \Delta J_{i,j}^{meas,+} = \Delta J_{i,j}^+ + e_{J(ij)} \\ \Delta J_{j,i}^{meas,+} = \Delta J_{j,i}^+ + e_{J(ji)} \end{cases} \quad (4)$$

In this set of equations, the superscript "*meas*" stands for measured phasors, and e is the corresponding measurement error. Fig. 3 shows an illustrative example of the faulted circuit, and (4) remains valid regardless of whether an IBR is installed at either terminal of the faulted line.

Let us assume p is the number of available synchrophasors at the control center. For these synchrophasors, an overdetermined set of linear equations can be formulated using (4) for each line as below:

$$\boldsymbol{m}_{p\times 1} = \boldsymbol{H}_{p\times(2+Nr)}\, \boldsymbol{x}_{(2+Nr)\times 1} + \boldsymbol{\varepsilon}_{p\times 1} \quad (5)$$

in which vectors $\boldsymbol{m}$ and $\boldsymbol{\varepsilon}$ denote the vector of superimposed measurements and the superimposed errors, respectively. Moreover, $\boldsymbol{H}$ denotes the coefficient matrix. The dimensions of these vectors are shown as subscripts. The vector $\boldsymbol{x}$ includes the

Authorized licensed use limited to: TU Delft Library. Downloaded on February 05,2024 at 10:49:11 UTC from IEEE Xplore. Restrictions apply.

unknown current sources representing the candidate line and all IBRs as follows:

$$\boldsymbol{x} = \begin{bmatrix} \Delta J_{i,j}^{+} & \Delta J_{i,j}^{+} & \Delta I_1^{+} \ldots & \Delta I_{Nr}^{+} \end{bmatrix}^T \quad (6)$$

The WLS method estimates the vector $\boldsymbol{x}$ to be:

$$\hat{\boldsymbol{x}} = (\boldsymbol{H}^{*}\boldsymbol{R}^{-1}\boldsymbol{H})^{-1}\boldsymbol{H}^{*}\boldsymbol{R}^{-1}\boldsymbol{m} \quad (7)$$

where $\boldsymbol{R}$ is the covariance matrix of superimposed errors, and the asterisk denotes the conjugate transpose operator. The *k*-th diagonal element of $\boldsymbol{R}$ is equal to the variance attributed to the error of the *k*-th superimposed measurement [15].

B. Identification of the Faulted Line

Equation set (5) can be formed for every line (assuming that the candidate line is truly faulted). Using the WLS method, the *WSSR* of every such line is minimized and calculated as below:

$$WSSR = [\boldsymbol{m} - \boldsymbol{H}\hat{\boldsymbol{x}}]^{*}\boldsymbol{R}^{-1}[\boldsymbol{m} - \boldsymbol{H}\hat{\boldsymbol{x}}] \quad (8)$$

For the faulted line, all measurements hold true in (5). Thus, the *WSSR* associated with the faulted line takes a zero value if measurements are error-free. Conversely, the *WSSR* of non-faulted lines takes non-zero values. This is because their coefficient matrices do not correspond to or have meaningful relations with the measurements taken [15]. Thus, the smallest *WSSR* obtained indicates the faulted line.

IV. Accounting for the High Penetration of IBRs

In the formulation just put forward, every IBR is modeled as a nodal current source in the positive-sequence superimposed circuit. The nodal current sources modeling the IBRs whose terminals are monitored by PMUs appear in both vectors $\boldsymbol{m}$ and $\boldsymbol{x}$ in (5). From linear algebra, including such variables in vector $\boldsymbol{x}$ does not create unsolvability concerns because its corresponding row in the matrix $\boldsymbol{H}$ has only one non-zero entry [23]. However, assuming a PMU at every IBR terminal may not be practical. Within this section, a technique is put forth to effectively diminish the quantity of unknown variables.

A. Rearranging the System of Equations

In this study, an IBR is called monitored if a PMU at its terminal measures its current and voltage synchrophasors. An unmonitored IBR refers to an IBR whose current/voltage synchrophasors are not taken by PMUs. The current sources replacing the faulted line and unmonitored IBRs are the only unknowns in (5) to be estimated by (7). This, however, will not be feasible when the number of unknowns in $\boldsymbol{x}$ exceeds the rank of $\boldsymbol{H}$ [15], [23]. The knowledge of the LVRT characteristics of IBRs can be exploited to overcome the preceding unsolvability concerns by reducing the number of unknowns. The number of monitored and unmonitored IBRs are denoted by Nm and Nn, respectively. The system of equations (5) can be rearranged as follows:

$$\boldsymbol{m}_{p\times 1}^{mod} = \boldsymbol{H}_{p\times(2+Nm)}^{mon}\,\boldsymbol{x}_{(2+Nm)\times 1}^{mon} + \boldsymbol{\varepsilon}_{p\times 1} \quad (9)$$

where

$$\boldsymbol{m}_{p\times 1}^{mod} = \boldsymbol{m}_{p\times 1} - \boldsymbol{H}_{p\times Nn}^{unm}\;\boldsymbol{x}_{Nn\times 1}^{unm} \quad (10)$$

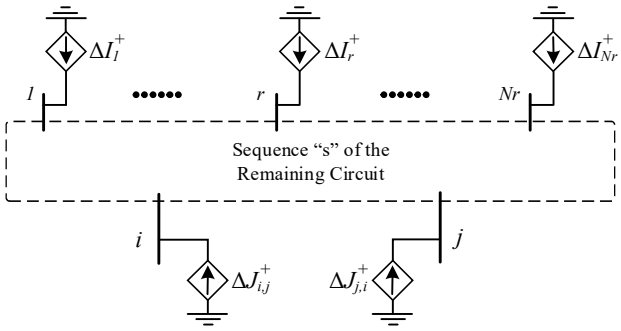

Fig. 3. Positive-sequence superimposed circuit following a fault on line *i*-*j*.

where $\boldsymbol{x}^{mon}$ contains the nodal current sources representing the candidate line, i.e., $\Delta J_{i,j}^{+}$ and $\Delta J_{j,i}^{+}$, plus those current sources representing the monitored IBRs. The matrix $\boldsymbol{H}^{mon}$ contains the coefficients corresponding to the variables in $\boldsymbol{x}^{mon}$. The vector $\boldsymbol{m}^{mod}$ is the modified measurement vector from which the contributions of the superimposed currents of unmonitored IBRs are excluded. Moreover, the vector $\boldsymbol{x}^{unm}$ only includes the superimposed currents of unmonitored IBRs, whose related coefficients are arranged in the matrix $\boldsymbol{H}^{unm}$.

In the proposed method, initially, the unknown currents resulting from unmonitored IBRs are not taken into consideration, which means $\boldsymbol{m}^{mod}$ is set equal to $\boldsymbol{m}$ in the first step. This enables us to calculate an initial estimation for the nodal currents representing the candidate line by solving (9). Then, an initial estimation of the positive-sequence superimposed voltage at the unmonitored IBRs' terminals can be obtained by (2). As will be detailed in subsection IV-B, the superimposed currents of unmonitored IBRs in $\boldsymbol{x}^{unm}$ can be approximated using their terminal voltage and LVRT characteristics. Then, $\boldsymbol{m}^{mod}$ is updated by (10). Next, the vector $\boldsymbol{x}^{mon}$ is also updated by solving (9). This process continues until the alterations in the vector $\boldsymbol{x}^{unm}$ caused by an iteration become insignificant. Finally, the *WSSR* for every line is calculated to identify the actual faulted line.

B. Modeling Unmonitored IBRs

The modified system of (9) only includes the superimposed nodal currents of the monitored IBRs and the nodal currents representing the candidate line. The solution of (9) gives the *WSSR* indices. This is irrespective of the number of unmonitored IBRs, whose contributions will be estimated separately based on their LVRT characteristics and incorporated in the formulation by (10). As a result, only two actual unknowns remain in (9) that represent the candidate line in the superimposed circuit. This is because other variables in $\boldsymbol{x}^{mon}$ are also present in the measurement vector. This approach eliminates the unsolvability concerns introduced by the presence of unmonitored IBRs, thus ensuring the solvability of the overall system of equations.

Under normal conditions, an IBR operates to inject both active and reactive power in accordance with its predetermined reference settings. The control references of IBRs during a fault are adjusted based on their terminal voltages and LVRT characteristics. In this regard, the LVRT characteristics of IBRs

Authorized licensed use limited to: TU Delft Library. Downloaded on February 05,2024 at 10:49:11 UTC from IEEE Xplore. Restrictions apply.

should meet the Grid Code requirements [21]-[22]. As shown in Fig. 2, the amount of voltage drop at an IBR terminal determines the required modification the IBR should apply to its reactive current injections. It is reasonable to assume that LVRT characteristics are available in the control center.

The positive-sequence superimposed current of an IBR connected to bus *r* is derived by subtracting the IBR's pre-fault current, denoted by $I_r^{+,pre}$, from its post-fault current, denoted by $I_r^{+,post}$. These currents can be obtained from:

$$I_r^{+,pre} = \frac{\left(P_{ref}^{pre} - jQ_{ref}^{pre}\right)}{\left(V_r^{+,pre}\right)^*} \tag{11}$$

$$I_r^{+,post} = \frac{\left(P_{ref}^{post} - jQ_{ref}^{post}\right)}{\left(V_r^{+,post}\right)^*} \tag{12}$$

where $V_r^{+,pre}$, P_{ref}^{pre}, and Q_{ref}^{pre} represent the pre-fault voltage at bus *r* in the positive-sequence circuit, and the active and reactive power references of the IBR, respectively. The superscript "*pre*" and "*post*" refer to the pre- and post-fault values, respectively. The pre-fault bus voltages are typically available in the control center as the output of state estimation methods [24]. The control center is assumed to know the pre-fault power references. Accordingly, $I_r^{+,pre}$ can be readily calculated using (11).

Obtaining $I_r^{+,post}$ from (12), however, is trickier as the post-fault voltage and power references are to be calculated. The post-fault voltage at bus *r* in the positive-sequence circuit can be calculated using the pre-fault voltage and the estimated superimposed voltage, i.e. $V_r^{+,post} = V_r^{+,pre} + \Delta V_r^+$. If $V_r^{+,post}$ lies within the dead band shown in Fig. 2, the post-fault power references (P_{ref}^{post} and Q_{ref}^{post}) will be the same as their pre-faults values (P_{ref}^{pre} and Q_{ref}^{pre}). Otherwise, the post-fault power references should be calculated using the IBR's LVRT characteristics as follows.

Let us assume that the phase-locked loops (PLLs) align the grid voltage to the *d*-axis. Thus, except for a short transient period following a fault, the positive-sequence *q*-axis voltage, i.e., v_q^+, will be zero in the pre- and post-fault conditions [1]. Accordingly, the pre- and post-fault positive-sequence voltage in the *d*-axis can be calculated as:

$$\begin{cases} v_d^{+,pre} = \left|V_r^{+,pre}\right| \\ v_d^{+,post} = \left|V_r^{+,post}\right| \end{cases} \tag{13}$$

where the operator |.| returns the amplitude of a phasor. Accordingly, the pre-fault reactive current of the IBR, i.e., $i_q^{+,pre}$, can be obtained as follows:

$$i_q^{+,pre} = \frac{-Q_{ref}^{pre}}{\left|V_r^{+,pre}\right|} \tag{14}$$

Let $f(V)$ denote the voltage support characteristic, which represents the change in the reactive current of the IBR in the positive-sequence circuit during faults, as shown in Fig. 2. Different IBRs might have different $f(V)$ characteristics. Using $f(V)$, $\Delta V_r^{+,post}$, and $i_q^{+,pre}$ obtained by (14), the post-fault reactive currents of the IBR following the fault onset can be obtained as below:

$$i_q^{+,post} = \text{Min}\left\{ i_q^{+,pre} + \overbrace{f(\Delta V_r^{+,post})}^{\Delta i_q^+},\ i_{max}^+ \right\} \tag{15}$$

where i_{max}^+ is the largest permissible current of the IBR in the positive-sequence circuit. The remaining current capacity of the IBR will be allocated to the active current generation. Due to the IBR's overcurrent limits, the active power generation of the IBR may have to be decreased to be able to inject the reactive current imposed by Grid Code requirements [21]-[22]. Accordingly, the post-fault active current of the IBR at instant *t* can be obtained as:

$$i_d^{+,post}(t) = \text{Min}\left\{ i_d^{+,pre},\ \sqrt{{i_{max}^+}^2 - {i_q^{+,post}}^2} \right\} \tag{16}$$

Using (13), the post-fault active and reactive power references of the IBR can be calculated from:

$$\begin{cases} P_{ref}^{post} = i_d^{+,post}\left|V_r^{+,post}\right| \\ Q_{ref}^{post} = -i_q^{+,post}\left|V_r^{+,post}\right| \end{cases} \tag{17}$$

The post-fault positive-sequence current of the IBR is obtained by replacing P_{ref}^{post} and Q_{ref}^{post} in (12). Finally, the superimposed current of the IBR is calculated by subtracting $I_r^{+,post}$ from $I_r^{+,pre}$.

TABLE I
LOCATIONS, SIZE, AND SETTINGS OF IBRS

Location (Bus No.)	Nominal Power	Voltage Support Slope	Operating References
1, 5, 7, 9, 12, 14, 15, 17, 24, 26, 3, 4, 8, 11, 13, 16, 18, 21, 27, 28	150 MVA	2	P_{ref}= 1 pu Q_{ref}= 0 pu

V. PERFORMANCE EVALUATION

Numerous fault cases are simulated on the IEEE 39-bus test system via the electromagnetic transient simulation tool in DIgSILENT PowerFactory with different IBR penetration levels. Table I tabulates the locations, rated power, and control references/settings of the set of 20 IBRs. The locations of PMUs are usually determined to establish network observability [25]. Hence, the method of [25] is used to place 12 PMUs at buses 3, 5, 8, 11, 14, 16, 19, 23, 25, 27, 29, and 39. The method's general performance is studied for various fault types across the system with different fault resistance. The method's accuracy for estimating the superimposed currents of unmonitored IBRs is studied. Next, the impact of input errors on the method's performance is scrutinized. Finally, the impact of various numbers, placement, and penetration levels of IBRs with different LVRT characteristics on the method's performance is investigated.

As defined in [26], the maximum acceptable total vector error (TVE) is 1% for phasor measurements. Therefore, the

Authorized licensed use limited to: TU Delft Library. Downloaded on February 05,2024 at 10:49:11 UTC from IEEE Xplore. Restrictions apply.

TABLE II
TVE (%) OF THE ESTIMATED SUPERIMPOSED CURRENT OF IBRS FOLLOWING DIFFERENT FAULTS AT 5% OF LINE 15-16

Fault Type	IBRs Location (Bus No.)												
	1	4	7	9	12	13	15	17	18	21	24	26	28
LLL*	1.29	1.26	1.88	0.60	0.80	0.24	1.89	4.36	4.48	1.42	3.41	1.96	2.23
SLG*	4.11	0.95	1.11	4.89	4.35	1.05	2.27	2.73	1.14	0.40	1.28	1.12	2.18
LL*	2.78	2.22	4.28	5.39	5.10	2.18	1.40	3.38	2.23	2.76	2.38	4.28	4.58
DLL*	2.59	1.97	4.07	4.78	4.32	1.62	1.72	2.97	3.27	3.42	1.99	4.82	3.37

* LLL: three phase, SLG: single phase to ground, LL: phase to phase, DLG: double phase to ground

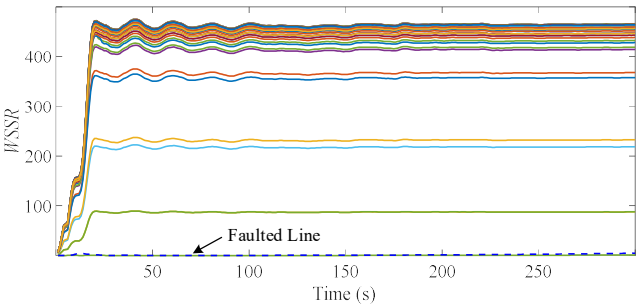

Fig. 4. *WSSRs* obtained for all lines over time after a solid SLG fault at 5% of line 15-16.

TABLE III
SUMMARY OF METHOD'S PERFORMANCE FOR DIFFERENT FAULTS

Fault Type	Index	Proposed Method			Method of [15]		
		0 Ω	20 Ω	50 Ω	0 Ω	20 Ω	50 Ω
LLL*	LIFR (%)	99.36	99.18	99.01	82.21	91.18	93.56
	AFDE (%)	0.49	0.68	0.89	11.12	6.23	4.86
SLG*	LIFR (%)	99.42	99.25	99.04	83.89	90.51	95.36
	AFDE (%)	0.48	0.98	1.32	16.13	5.41	4.12
DLG*	LIFR (%)	99.43	99.02	98.96	84.19	91.86	95.17
	AFDE (%)	0.62	0.79	0.94	14.68	3.41	2.79

* LLL: three phase,
* SLG: single phase to ground,
* DLG: double phase to ground

phasors are contaminated with errors to have TVEs with random phase angles between 0 and π, and random amplitudes evenly distributed between 0% and 1%. The method's performance with higher measurement errors is investigated in subsection V-B.

A. Method's General Performance

The method takes the unmonitored IBRs into account by estimating their superimposed currents and modifying the measurement vector using (10). To achieve this, the post-fault terminal voltages of these IBRs are used to obtain their post-fault active and reactive power references by (14) to (17). Table II reports the TVEs between the true and estimated positive-sequence superimposed currents of the unmonitored IBRs at 80 ms following a solid SLG fault at 5% of line 15-16. The achieved maximum TVE is below 5%, indicating the good performance of the proposed method in accurately computing the superimposed currents of unmonitored IBRs.

As explained, the fault current contributions of unmonitored IBRs are initially disregarded by the proposed method. This leads to errors in the computations initially, subsequently leading to an increased *WSSR* value for the faulted line. In each iteration, the superimposed currents of unmonitored IBRs are estimated, updated, and used as the starting point of the next iteration. The main objective of this iterative procedure is to enhance the precision of the proposed method. As a result, more accurate calculations of fault distance can be obtained, along with a reduced value for the *WSSR* of the faulted line. If unmonitored IBRs are disregarded, the fault distance for the fault at 5% of the line length is calculated at 0.87%. However, this is obtained at 4.73% after applying the proposed method. Fig. 4 shows the *WSSRs* of all lines over time following the fault onset, in which the faulted line's *WSSR* is noticeably smaller than those of non-faulted lines.

TABLE IV
METHOD'S SENSITIVITY TO INPUT ERRORS

Error Source	Results	Variation Range of Errors (%)				
		±1	±2	±3	±4	±5
Measured Phasors	FLISR (%)	99.52	99.31	99.11	98.96	98.71
	AFDE (%)	0.56	0.63	0.71	0.82	1.02
Generator Parameters	FLISR (%)	99.45	99.34	99.28	99.11	99.03
	AFDE (%)	0.63	0.69	0.75	0.89	0.99
Line Parameters	FLISR (%)	99.15	98.95	98.56	98.01	97.36
	AFDE (%)	0.75	0.99	1.63	2.23	2.91

TABLE V
METHOD'S SENSITIVITY TO IBR PENETRATION LEVELS AND DISTRIBUTIONS

IBRs' Penetration	Results	Number of IBRs			
		24	20	16	12
50%	FLISR (%)	99.53	99.48	99.54	99.39
	AFDE (%)	0.57	0.55	0.52	0.55
65%	FLISR (%)	99.39	99.43	99.49	99.52
	AFDE (%)	0.6	0.63	0.61	0.64
80%	FLISR (%)	99.21	99.14	99.16	99.11
	AFDE (%)	0.63	0.65	0.64	0.71

The method of [15] is applicable against all fault types and has better features compared to existing methods in the literature, as per the comprehensive review of the existing WABP methods in [10]. Thus, a performance comparison is presented for the proposed method and that of [15]. In this regard, various fault types are studied at 40 evenly distributed distances on every line with 0 Ω, 20 Ω and 50 Ω of fault resistance. The *WSSR* index and the calculated fault distance are the criteria employed for the identification of the faulted line. Simulations show that the precision of faulted-line identification is more affected by the fault current contribution of IBRs following faults closer to substations. Hence, the results are only reported for faults within 0% to 20% and 80% to 100% of line lengths. Table III tabulates the obtained results in terms of average fault distance error (AFDE) and faulted-line identification success rate (FLISR). The average value obtained for fault distance between 80 ms and 120 ms following the fault onset is used to calculate AFDE. The method is successful in more than 99% of the simulated cases in identifying the faulted line providing higher accuracy in the fault distance calculation. Disregarding the presence of IBRs results in a larger *WSSR* for the faulted line and introduces excessive errors in the fault distance calculations. These are the reasons that the existing method leads to a noticeably lower success rate and accuracy as compared with the proposed method.

Authorized licensed use limited to: TU Delft Library. Downloaded on February 05,2024 at 10:49:11 UTC from IEEE Xplore. Restrictions apply.

B. Method's Sensitivity to Input Errors

The method's sensitivity to input errors is evaluated by simulating 200 arbitrary faults across the transmission grid. Phasors and parameters are contaminated with normally distributed errors of mean zero. The three-sigma criterion is used to report the error ranges. The procedure is repeated 500 times for each fault case with random input errors, and the obtained results are tabulated in Table IV. As can be seen, with up to 5% errors in the measurements, the method's success rate remains more than 98.83%. The effectiveness of the WLS method in managing measurement errors arises from its utilization of the redundancy of the equations to diminish the overall impact of these errors. The outcomes acquired from the inclusion of errors in generator and transmission line parameters are summarized in Table IV. As anticipated, the method's accuracy and success rate experience a slight decline with an increase in the range of parameter errors.

C. Impact of IBR Locations and Control Strategies

The method performs well, regardless of the number, location, and LVRT characteristics of IBRs. To demonstrate this, three different penetration levels are studied. A total of 100 random placements of IBRs are considered for each penetration level and number of IBRs. The nominal powers of IBRs are adjusted in accordance with their quantity and the desired level of penetration. Table V reports the FLISR and AFDE indices obtained for the same 200 fault cases selected in subsection V-B. It can be concluded that the method's performance is not noticeably affected by the penetration level, control settings, and location of IBRs.

VI. Conclusion

This paper proposes an effective superimposed-circuit-based wide-area backup protection method for transmission lines in the presence of inverter-based resources (IBRs). The weighted least-squares method is utilized to solve the system of equations formulated. Potential solvability issues are minimized by excluding the currents of unmonitored IBRs (those without PMUs) from the set of unknowns. It is demonstrated that the presence of these IBRs can easily be taken into account using the *Substitution Theorem* and the IBRs' low-voltage ride-through (LVRT) characteristics. The faulted line is readily identified by comparing the weighted sum of squared residuals calculated for candidate lines. The method can readily take into account any LVRT characteristics imposed upon IBRs by the Grid Code. As verified by simulation studies, the method is robust against measurement and parameter errors. For different IBR penetration levels, numbers, locations, and LVRT characteristics, the proposed WABP method is shown to outperform existing methods irrespective of fault type, resistance, and location.

References

[1] A. Yazdani and R. Iravani, *Voltage-Sourced Converter in Power Systems: Modelling, Control, and Application*. New York, NY, USA: Wiley, 2010.

[2] V. Telukunta, J. Pradhan, A. Agrawal, M. Singh, and S. G. Srivani, "Protection challenges under bulk penetration of renewable energy resources in power systems: A review," *CSEE J. of Power and Energy Syst.*, vol. 3, no. 4, pp. 365-379, Dec. 2017.

[3] J. Hossain and A. Mahmud, Renewable Energy Integration: Challenges and Solutions. Singapore: Springer-Verlag, 2014.

[4] O. H. Gupta, M. Tripathy, and V. K. Sood, *Protection Challenges in Meeting Increasing Electric Power Demand*. Springer International Publishing, Jan, 2021.

[5] S. H. Horowitz and A. G. Phadke, *Power System Relaying*. 4th ed. John Wiley & Sons, 2008.

[6] J. L. Blackburn and T. J. Domin, *Protective Relaying: Principles and Applications*, Florida, USA: CRC Press, 2014.

[7] Y. Fang, K. Jia, Z. Yang, Y. Li, and T. Bi, "Impact of inverter-interfaced renewable energy generators on distance protection and an improved method," *IEEE Trans. Ind. Electron.*, vol. 66, no. 9, pp. 7078-7088, Sep. 2019.

[8] Z. Yang, W. Liao, H. Wang, C. L. Bak and Z. Chen, "Improved Euclidean distance based pilot protection for lines with renewable energy sources," *IEEE Trans. Ind. Informat., Early access*.

[9] M. Popov *et al.*, "Enhancing distance protection performance in transmission systems with renewable energy utilization," *2020 IEEE PES Innovative Smart Grid Technologies Europe*, 2020, pp. 181-185.

[10] S. Azizi, M. R. Jegarluei, J. S. Cortes, V. Terzija, State of the art, challenges and prospects of wide-area event identification on transmission systems, *Int. J. of Electr.Power & Energy Syst*, vol. 148, 2023.

[11] M. Majidi, M. Etezadi-Amoli, M. S. Fadali, "A sparse-data-driven approach for fault location in transmission networks," *IEEE Trans. Smart Grid*, vol. 8, no. 2, pp. 548-556, Mar. 2017.

[12] M. K. Neyestanaki and A. M. Ranjbar, "An adaptive PMU-based wide area backup protection method for power transmission lines," *IEEE Trans. Smart Grid*, vol. 6, no. 3, pp. 1550–1559, May 2015.

[13] G. Zhang, X. Tong, Q. Hong, X. Lu, and C. D. Booth, "A novel fault isolation method in power system with dynamic topology using wide-area information," *IEEE Trans. on Ind. Informat.*, vol. 18, no. 4, pp. 2399-2410, April 2022.

[14] J. J. Chavez et al., "Non-homogeneous sampling rate wide Area Backup protection using synchrophasors and IED data," *International Conference on Smart Grid Synchronized Measurements and Analytics (SGSMA)*, pp. 1-7, May 2022.

[15] S. Azizi and M. Sanaye-Pasand, "From available synchrophasor data to short-circuit fault identity: Formulation and feasibility analysis," *IEEE Trans. Power Syst*., vol. 32, no. 3, pp. 2062-2071, May 2017.

[16] S. Azizi, G. Liu, A. S. Dobakhshari, and V. Terzija "Wide-area backup protection against asymmetrical faults using available phasor measurements," *IEEE Trans. Power Del*., vol. 35, no. 4, pp. 2032-2039, Aug. 2020.

[17] A. S. Dobakhshari and A. M. Ranjbar, "A wide-area scheme for power system fault location incorporating bad data detection," *IEEE Trans. Power Del.*, vol. 30, no. 2, pp. 800-808, April 2015.

[18] M. R. Jegarluei, A. S. Dobakhshari, and S. Azizi, "Reducing the computational complexity of wide-area backup protection in power systems," *IEEE Trans. Power Del*., vol. 37, no. 3, pp. 2421-2424, Jun.

[19] S. Biswal, S. D. Swain, R. D. Patidar, A. K. Bhoi, and O. P. Malik, "Integrated wide-area backup protection algorithm during stressed power system condition in presence of wind farm," *Arabian J. for Science and Engineering*, vol. 46, no. 10, pp 9363-9376, 2021.

[20] M. R. Jegarluei, P. Aristidou, and S. Azizi, "Wide-Area backup protection against asymmetrical faults in the presence of renewable energy sources," *Int. J. of Electr.Power & Energy Syst.*, vol. 144, 2023.

[21] H. Berndt, M. Hermann, H. D. Kreye, R. Reinisch, U. Scherer, and J. Vanzetta, "Network and system rules of the German transmission system operators," *Verband der Netzbetreiber*, Germany, Tech. Rep., 2007.

[22] *The Grid Code*, National Grid Electricity System Operator Limited, Jun. 2022. [Online]. Available: https://www.nationalgrideso.com/document/162271/download.

[23] C. D. Meyer, *Matrix Analysis and Applied Linear Algebra*. Philadelphia, PA, USA: SIAM, 2001.

[24] A. S. Dobakhshari, S. Azizi, M. Paolone, and V. Terzija, "Ultra-fast linear state estimation utilizing SCADA measurements," *IEEE Trans. Power Syst*., vol. 34, no. 4, pp. 2622–2631, Jul. 2019.

[25] S. Azizi, A. S. Dobakhshari, S. A. N. Sarmadi, and A. M. Ranjbar, "Optimal PMU placement by an equivalent linear formulation for exhaustive search," *IEEE Trans. Smart Grid*, vol. 3, no. 1, pp. 174–182, Mar. 2012.

[26] *IEEE Standard for Synchrophasor Measurements for Power Systems*, IEEE Std. C37.118.1-2011, 2011.

Authorized licensed use limited to: TU Delft Library. Downloaded on February 05,2024 at 10:49:11 UTC from IEEE Xplore. Restrictions apply.